

***Caenorhabditis elegans* AGXT-1 is a mitochondrial and ~~cold~~temperature-adapted ortholog of peroxisomal human AGT1: New insights into between-species divergence in glyoxylate metabolism.**

Noel Mesa-Torres^{1*†}, Ana C. Calvo^{2†}, Elisa Oppici³, Nicholas Titelbaum^{1,2}, Riccardo Montioli³, Antonio Miranda-Vizuete⁴, Barbara Cellini³, Eduardo Salido⁵ and Angel L. Pey^{1*}.

¹ Department of Physical Chemistry, Faculty of Sciences, University of Granada, Av. Fuentenueva s/n, 18071 Granada, Spain.

² Program in Cellular Neuroscience, Neurodegeneration, and Repair, Department of Cell Biology, Yale University School of Medicine, New Haven, CT 06536, USA.

³ Department of Neurological, Biomedical and Movement Sciences, Section of Biological Chemistry, University of Verona, Strada Le Grazie 8, 37134 Verona, Italy.

⁴ Instituto de Biomedicina de Sevilla, Hospital Universitario Virgen del Rocío/Consejo Superior de Investigaciones Científicas / Universidad de Sevilla, 41013 Sevilla, Spain.

⁵ Centre for Biomedical Research on Rare Diseases (CIBERER), University Hospital of the Canary Islands, and CIBICAN, University of La Laguna, 38320 Tenerife, Spain

Abstract

In humans, glyoxylate is an intermediary product of metabolism, whose concentration is finely balanced. Mutations in peroxisomal alanine:glyoxylate aminotransferase (hAGT1) cause primary hyperoxaluria type 1, which results in glyoxylate accumulation that is converted to toxic oxalate. In contrast, glyoxylate is used by the nematode *C. elegans* through a glyoxylate cycle to by-pass the decarboxylation steps of the tricarboxylic acid cycle and thus contributing to energy production and gluconeogenesis from stored lipids. To investigate the differences in glyoxylate metabolism between humans and *C. elegans* and to determine whether the nematode might be a suitable model for PH1, we have characterized here the predicted nematode ortholog of hAGT1 (AGXT-1) and compared its molecular properties with those of the human enzyme. Both enzymes form active PLP-dependent dimers with high specificity towards alanine and glyoxylate, and display similar

* Corresponding authors: noelmesatorres@gmail.com, angelpay@ugr.es

† These authors contributed equally to this work

three-dimensional structures. Interestingly, AGXT-1 shows 5-fold higher activity towards the alanine/glyoxylate pair than hAGT1. Thermal and chemical stability of AGXT-1 is lower than that of hAGT1, suggesting ~~cold~~temperature-adaptation of the nematode enzyme linked to the lower optimal growth temperature of *C. elegans*. Remarkably, *in vivo* experiments demonstrate the mitochondrial localization of AGXT-1 in contrast to the peroxisomal compartmentalization of hAGT1. Our results support the view that the different glyoxylate metabolism in the nematode is associated with the divergent molecular properties and subcellular localization of the alanine:glyoxylate aminotransferase activity.

Keywords. Primary hyperoxaluria; enzyme kinetics; substrate specificity; protein stability; conformational disease.

1 1. Introduction

2 Glyoxylate is an intermediary product of metabolism in humans, which is formed
3 from precursors such as glycine, glycolate, hydroxypyruvate and hydroxyproline. Among
4 mammals, alanine:glyoxylate aminotransferase (AGT) protein compartmentalization is
5 linked to metabolism of glyoxylate precursors, varying from mainly mitochondrial in
6 carnivorous, peroxisomal in herbivorous and located in both organelles in omnivorous [1].
7 The human *AGXT* gene encodes an alanine:glyoxylate aminotransferase enzyme (hAGT1;
8 E.C. 2.6.1.44) that is responsible for glyoxylate detoxification in peroxisomes of
9 hepatocytes [2] thus balancing the glyoxylate concentration. The human genome encodes
10 a second protein with alanine:glyoxylate aminotransferase activity named hAGT2 [3] that
11 catalyses multiple aminotransferase reactions [4,5] and might be involved in the
12 metabolism of glyoxylate within the mitochondria. hAGT1 is a pyridoxal 5'-phosphate
13 (PLP)- dependent enzyme that catalyses the amino transfer from L-alanine to glyoxylate

14 resulting into pyruvate and glycine and this reaction is largely shifted towards glycine
15 formation [6]. Mutations in *AGXT* gene cause primary hyperoxaluria type 1 (PH1), an error
16 of amino acid metabolism inherited in an autosomal recessive manner [2]. PH1 results in
17 the accumulation of glyoxylate in hepatocytes where it is oxidized to oxalate (a metabolic-
18 end product in humans) causing progressive renal failure and ultimately leading to a build-
19 up of oxalate and life-threatening oxalate precipitation [2,7]. Currently, the best method to
20 treat PH1 is a double liver and kidney transplantation, but this treatment often shows
21 significant rates of morbidity and mortality.

22 After the complete sequencing of *Caenorhabditis elegans* genome, early
23 estimations indicated that around 74% of human gene sequences had nematode
24 counterparts [8]. Therefore, a lot of effort was put into identifying potential nematode
25 orthologs to human genes. As a result, using an *in silico* search of genes associated with
26 inborn errors of metabolism in humans, an open-reading frame termed as *T14D7.1* was
27 predicted as an ortholog of human *AGXT* gene [9]. The *T14D7.1* gene (now renamed as
28 *agxt-1*) is located on chromosome 2 and it is organized into 11 exons
29 (WBGene00011767), whose conceptual translation results into a 405 amino acids protein
30 (AGXT-1). Unlike humans, the nematode *C. elegans* has an active glyoxylate cycle (GC)
31 [10] that allows to bypass the decarboxylation steps of the tricarboxylic acid (TCA) cycle
32 [11], thus linking catabolic and biosynthetic capacities. In the nematode, the key enzyme
33 of this cycle is a single bi-functional enzyme (ICL-1), which has isocitrate lyase activity (N-
34 terminal domain) and malate synthase activity (C-terminal domain) [12] that are regulated
35 in a developmentally specific manner [13,14].

36 We herein present data supporting that the divergent glyoxylate metabolism
37 between humans and the nematode *C. elegans* could ~~be linked to~~involve different
38 molecular properties and subcellular localization of their respective AGT enzymes. Further,

39 we demonstrate that even though AGXT-1 and hAGT1 proteins have similar quaternary
40 structure and substrate specificities, AGXT-1 displays higher specific activity and lower
41 protein stability, possibly reflecting ~~cold~~ temperature adaptation of the nematode enzyme.
42 *In vivo* studies demonstrate the mitochondrial localization of AGXT-1 in contrast to the
43 peroxisomal functional environment of hAGT1. In this work, we provide novel insights into
44 the evolutionary changes in protein stability, roles of AGT proteins and the divergence of
45 glyoxylate metabolism between vertebrates and invertebrates.

46 **2. Materials and Methods**

47 ***C. elegans* AGXT-1 cloning, expression and purification.** The *agxt-1* ORF was
48 amplified from a *C. elegans* cDNA library and cloned into a pET-28 (Novagen) vector using
49 the primers ACAGCTAGCATGCAGCCAACAGGGAATCAAATA and TATGTCGACTTAA-
50 ACCAAATTAGGATCCGATGGACTT forward and reverse respectively and restriction
51 enzymes NheI-HF and Sall-HF (New England Biolabs). This construct incorporates a His-
52 tag sequence at the N-terminal domain of AGXT-1. *E. coli* BL21(DE3) competent cells
53 were transformed with the plasmid and were grown in LB medium supplemented with 30
54 $\mu\text{g}\cdot\text{ml}^{-1}$ kanamycin. Overnight cultures were diluted 40-fold in fresh LB-kanamycin for 3 h
55 at 37°C and induced at 4°C by adding IPTG 0.5 mM for 8 h. Cells were harvested and
56 lysed by sonication in binding buffer (20 mM NaH_2PO_4 , 200 mM NaCl, 50 mM imidazole,
57 pH 7.4) supplemented with protease inhibitors (EDTA-free protease inhibitor cocktail,
58 Roche). Soluble extracts obtained after ultracentrifugation at 70,000 x g were loaded onto
59 an IMAC columns (GE Healthcare) and eluted with binding buffer supplemented with 500
60 mM imidazole. His-AGXT-1 was further purified by size exclusion chromatography using a
61 HiLoadTM 16/60 SuperdexTM 200 column running in 20 mM Hepes (2-[4-(2-
62 hydroxyethyl)piperazin-1-yl]ethanesulfonic acid), 200 mM NaCl, pH 7.4. The concentration
63 of His-AGXT-1 (hereafter AGXT-1) protein was evaluated using a sequence-based

64 extinction coefficient of $0.763 \text{ ml}\cdot\text{mg}^{-1}\cdot\text{cm}^{-1}$ at 280 nm [15]. The purification of hAGT1 was
65 performed as described previously [16]. Isolation of apo-forms of both enzymes was
66 attempted by using the protocol previously described [17]. PLP concentration was
67 calculated by using a molar extinction coefficient of $4,900 \text{ M}^{-1}\cdot\text{cm}^{-1}$ at 388 nm [18].

68 **Spectroscopic analyses.** All the spectroscopic assays were performed in a 20 mM
69 HEPES, 200 mM NaCl, pH 7.4 buffer at 25°C. UV-visible absorption spectroscopy was
70 performed in an Agilent 8453 diode-array spectrophotometer using cuvettes with a path
71 length of 3 mm and 20 μM protein (in subunit). Near-UV/visible circular dichroism
72 measurements were performed in a Jasco J-710 spectropolarimeter by using 5-mm path
73 length cuvettes with 20 μM protein (in subunit). Dynamic light scattering was carried out
74 using a protein concentration of 5 μM (in subunit) in the presence of 50 μM PLP in a
75 Zetasizer Nano ZS (Malvern Inc.) with 3-mm path length cuvettes and applying the Stokes-
76 Einstein equation assuming a spherical shape for the scattering particles.

77 **Enzyme activity measurements.** The overall transaminase activity was measured at
78 37°C with a protein concentration of $2.5 \mu\text{g}\cdot\text{ml}^{-1}$ in the presence of 150 μM PLP in 0.1 M
79 phosphate buffer pH 8. The time of the reaction was 2 minutes and the substrate
80 concentration was 0.25-2 mM glyoxylate and 0-100 mM L-alanine. Pyruvate formation was
81 evaluated following the oxidation of NADH at 340 nm by a coupled enzyme assay using
82 lactate dehydrogenase [19] during 3 minutes at 37°C. Global fittings were performed
83 according to a double-displacement mechanisms [6,16]. To determine the pH
84 dependence, activity measurements were performed using this coupled assay in the
85 presence of 2 mM glyoxylate and 100 mM L-alanine at 37°C in the following buffers: 100
86 mM HEPES (pH 7-8), MES (2-(N-morpholino)ethanesulfonic acid, pH 6-6.5), acetate (pH
87 4.5-5.5) or formate (pH 3-4). The time of the transamination reaction was set at 1.5
88 minutes (pH 7-8), 4 minutes (pH 6-6.5) and 10 minutes (pH 3.5-5.5). The dependence of

89 specific activity on temperature was measured at 15, 20, 25, 30 and 37°C with reaction
90 times from 2 to 10 minutes. To investigate the substrate specificity, the overall
91 transamination reaction was measured in the presence of different amino acids (L-alanine,
92 L-serine, L-arginine, L-glutamate, L-aspartate and L-phenylalanine) and ketoacids
93 (glyoxylate and pyruvate) by incubating the enzymes (2.5-100 $\mu\text{g}\cdot\text{ml}^{-1}$) with the amino acid
94 at 100 mM, the ketoacid at 2 mM and in the presence of 200 μM PLP in 0.1 M phosphate
95 buffer, pH 8 and 37°C. Aliquots of each reaction mixture were collected at various times
96 and the reaction was stopped by adding 10% (w/v) trichloroacetic acid. The amount of
97 ketoacid consumed was determined by HPLC after derivatization with 2,4-
98 dinitrophenylhydrazine as previously described [20].

99 **Differential scanning calorimetry.** DSC experiments were performed and analysed as
100 previously described for hAGT1 [17,21]. Briefly, the model considers the irreversible
101 denaturation of the native protein to a final state that cannot fold back, and this kinetic
102 conversion is characterized by a first-order rate constant k , which changes with
103 temperature according to the Arrhenius equation. The half-life at any temperature can thus
104 be obtained from extrapolation of k to a given temperature following the Arrhenius plot and
105 determined as $t_{1/2} = \ln(2)/k$.

106 **Urea denaturation.** Urea denaturation of AGXT-1 and hAGT1 was performed by
107 incubating the enzymes (5 μM in protein subunit) in 20 mM Hepes, 200 mM NaCl, 1mM
108 TCEP (Tris(2-carboxyethyl)phosphine) pH 7.4 with urea at concentrations ranging from 0-8
109 M. Urea concentration was determined by refractive index measurements. Samples were
110 incubated at 25°C for 16 h and then denaturation was monitored by Far-UV circular
111 dichroism spectroscopy (200-260 nm; 1 mm quartz cuvettes). Refolding experiments were
112 performed by dilution of protein samples denatured in 8 M urea solution with urea-free

113 buffer and allowed to equilibrate at 25°C for 4 h prior to Far-UV CD spectroscopic
114 analyses.

115 **Structural modelling.** The structural model of AGXT-1 protein was obtained using the
116 Modeler v9.13 software, the AGXT-1 amino acids sequence and the crystal structure of
117 human hAGT1 (pdb 1H0C) protein as a template. The model refinement was performed by
118 energy minimization applying the CHARM27 force field of the MOE software. The
119 adjustment of the protonation state, the coordinate based isoelectric point calculation, the
120 electrostatic surface map drawing, the structural alignment and the images construction
121 were performed using MOE 2013 software (CCG group).

122 **Strains.** *C. elegans* worms were culture and handle as described before [22]. The
123 following strains were used: wild type N2 Bristol, UGR1 *alpEx1 [Pmyo-3::tomm-20:: gfp,*
124 *Pmyo-3::agxt-1(50aa)::tagrfp, Punc-122::gfp]*, UGR3 *alpEx3 [Pmyo-3:: tomm -20:: gfp,*
125 *Pmyo-3::agxt-1(100aa):: tagrfp, Punc-122:: gfp]* UGR7 *alpEx7 [Pmyo-3:: tomm -20:: gfp,*
126 *Pmyo-3:: tagrfp, Punc-122:: gfp]*.

127 **Molecular biology and transgenic lines.** The nucleotide sequence corresponding to the
128 first 50 and 100 amino acids of the *agxt-1* cDNA sequence were amplified and cloned into
129 a gateway plasmid pDONR221 These clones were fused in frame with tagRFP and the
130 *unc-54* gene 3-UTR and expressed under the *myo-3* promoter, using the Multi Site
131 Gateway Pro Plus Kit (ThermoFisher, catalogue number 11791-100 and 11789-013).
132 These plasmids were injected at 5 ng· μl^{-1} together with a plasmid expressing the
133 mitochondrial fusion construct TOMM-20::GFP under the control of the same *myo-3*
134 promoter (kindly provided by Dr. Marc Hammarlund, Yale University) at 5 ng· μl^{-1} and the
135 co-injection marker *Punc-122::gfp*. Transgenic animals were generated using standard
136 techniques [23].

137 **Fluorescence and confocal image acquisition and analysis.** Images of fluorescence
138 fusion proteins were taken in live adults *C. elegans* nematodes using a 60X CFI Plan Apo
139 VC, numerical aperture 1.4, oil-immersion objective on an UltraView VoX spinning-disc
140 confocal microscope (PerkinElmer Life and Analytical Sciences). Worms were
141 synchronized 3 days prior to experiment, and first day of adulthood animals were
142 analysed. Animals were immobilized during image acquisition using 10 μ M Levamisol
143 (Sigma). Images were analysed using Volocity software (Improvision).

144 **3. Results**

145 **AGXT-1 is a mitochondrial protein.** According to a protein sequence comparison, *C.*
146 *elegans* AGXT-1 shows much higher identity/similarity to peroxisomal hAGT1 protein than
147 to mitochondrial hAGT2, which has a different fold (Table 1). The sequence of AGXT-1 is
148 13 residues longer than hAGT1 and all catalytic residues involved in the binding and
149 stabilization of the coenzyme at the active site are conserved in both proteins (Figure 1,
150 red highlighted residues) [24]. However, we also found two interesting differences between
151 the two primary sequences (Figure 1, green highlighted residues). First, the 13 extra
152 residues of AGXT-1 protein are located in the N-terminal domain. Mitochondrial targeting
153 sequences (MTS) usually consist of 20-60 residues in the N-terminal domain that are
154 prone to form an amphipathic alpha helix [25]. Bioinformatics tools, such as MitoProt [26]
155 or TargetP 1.1 Server [27], predict probabilities of 75-85% for the N-terminal domain of
156 AGXT-1 to form a cleavable amphipathic alpha helix consistent with a potential MTS.
157 Second, the AGXT-1 protein lacks the C-terminal tripeptide that constitutes the
158 peroxisomal targeting sequence type 1 (PTS1) required for hAGT1 peroxisomal import
159 through Pex5p-dependent route [28,29], which is conserved between humans and
160 nematodes [30]. *C. elegans* also lacks the alternative PTS2 pathway to target proteins to

170 This could be a consequence of either a non-proper folding of tagRFP and/or the high
171 level of expression of the recombinant protein. To avoid this aggregation issue, we
172 generated additional transgenic strains expressing only the fusion of the N-terminal
173 sequence of AGXT-1 (containing the putative MTS) with tagRFP. We generated two
174 different transgenic strains expressing the first 50 and 100 amino acids of AGXT-1 fused in
175 frame with tagRFP. As mitochondrial marker, we used a transgenic strain expressing a
176 TOMM-20::GFP fusion protein [37,38]. When tagRFP was expressed alone (Figure 2a), a
177 diffused cytosolic pattern was seen (Figure 2c), compared with the mitochondrial
178 localization of TOMM-20::GFP protein (Figure 2b). However, tagRFP fused to either the
179 first 50 or 100 amino acids of AGXT-1 (Figure 2e-i), was targeted to mitochondria (Figure
180 2g-k), as demonstrated by the colocalization with TOMM-20::GFP (Figure 2h-l). These
181 data confirm that the N-terminus of AGXT-1 encodes a functional MTS, thus reinforcing
182 the idea of AGXT-1 being a mitochondrial enzyme in *C. elegans*.

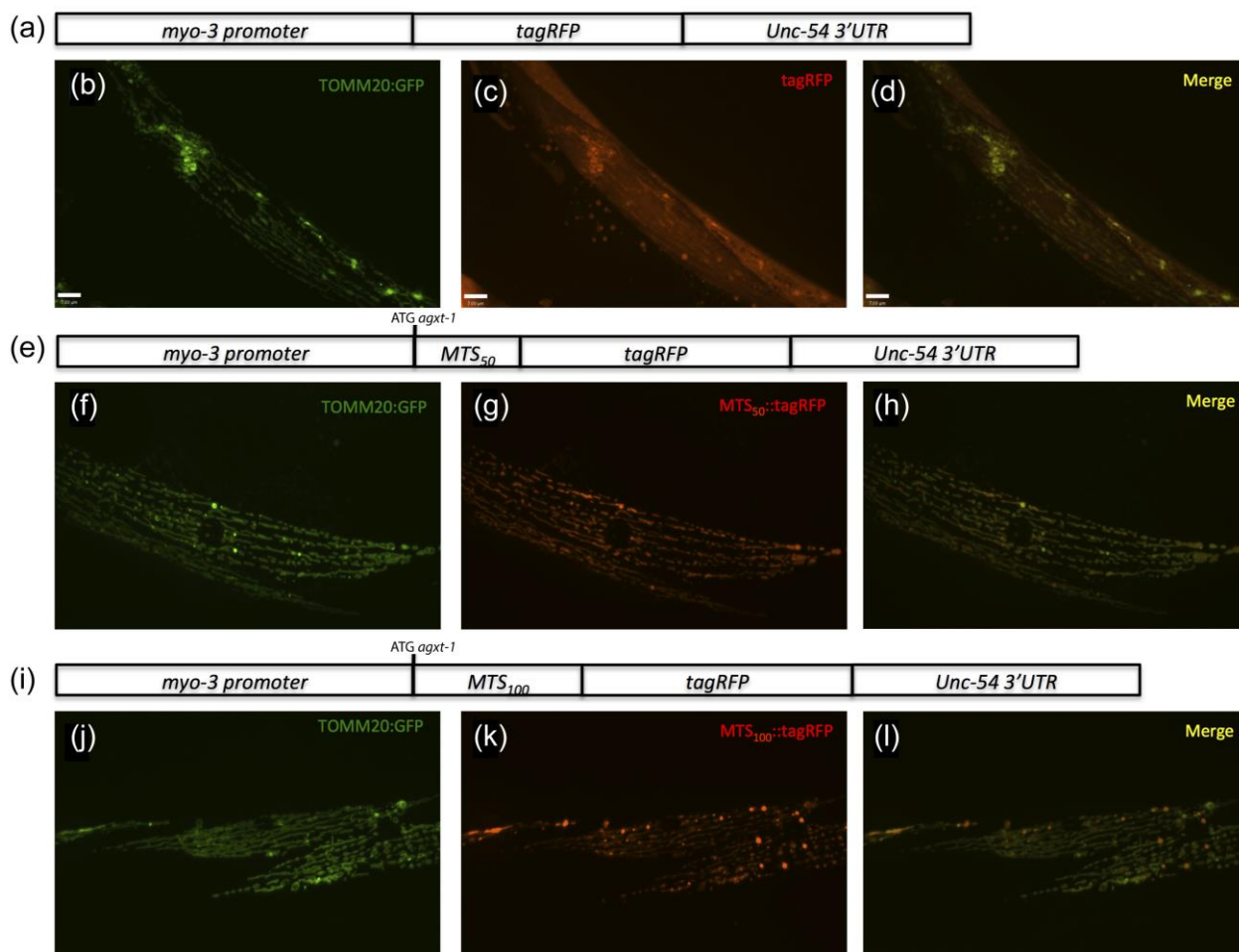


Figure 2. **Mitochondrial localization of AGXT-1.** Cartoons representing the DNA constructs used to express tagRFP (a), the first 50 amino acids (e) and the first 100 amino acids (i) of AGXT-1 fused to tagRFP under the control of the *myo-3* promoter along with the *unc-54* 3'-UTR. TOMM-20::GFP expression is found with the typical tubular mitochondrial pattern in muscle cells (b, f and j). When tagRFP is expressed alone, a diffused cytosolic pattern is seen (c) and no colocalization is found with TOMM-20::GFP (d, merge). Fusing the first N-terminal 50 (MTS₅₀) (g) or 100 (MTS₁₀₀) (k) amino acids of the AGXT-1 to tagRFP targets the protein to mitochondria. The GFP and tagRFP fluorescence now colocalize to the same organelle (h and l, merge).

183 **AGXT-1 and hAGT1 share overall structure.** Taking into account the considerable
 184 sequence homology between AGXT-1 and hAGT1, we built a structural homology model
 185 of AGXT-1 using the available crystal structure of hAGT1 as a template [24]. Due to the
 186 high flexibility of the N-terminus of hAGT1 and substantial sequence differences between
 187 the N-terminal domains of both proteins (Figure 1), we did not include in the structural

188 alignment the first 38 and 23 amino acids of AGXT-1 and hAGT1, respectively. The AGXT-
189 1 model was subsequently refined by energy minimization. The superposition of the
190 obtained AGXT-1 model and the hAGT1 structure predicts that the two proteins share a
191 similar overall conformation and secondary structure composition (Figure 3a). The binding
192 mode of PLP to AGXT-1 protein appears to be very similar to that of the human enzyme
193 and involves a Schiff base linkage with Lys226, a base stacking hydrophobic interaction
194 between the pyridine ring and the side chain of Trp125, a salt bridge between the N1 of
195 PLP and Asp200, an H-bond of the 3'OH group of PLP and Ser175 and several H-bonds
196 between the phosphate group of the coenzyme and Gln225, Gly99 and His100 (Figure
197 3b). Moreover, two interchain contacts of the phosphate group of PLP in hAGT1 with
198 Tyr260 and Thr263 of the neighbouring subunit, are probably held by Tyr277 and Thr280
199 in AGXT-1.

200 However, some differences are visible in the active site region and on the protein
201 surface. As for the active site cleft, Ser81 that in hAGT1 is critical for PLP binding [39] is
202 replaced by a threonine residue (Thr98) in AGXT-1. Moreover, Arg360, whose side chain
203 binds the carboxylate group of the substrate in hAGT1 [24], is replaced by Ile377 in AGXT-
204 1 (Figure 3c), thus leading to a different active site polarity and possibly a different
205 substrate binding mode. In addition, Trp246 and Met259 of hAGT1 are replaced by Glu263
206 and Arg276 in AGXT-1. As shown in Figure 3d, these two charged residues could interact
207 by a salt bridge, thus probably stabilizing the interface loop 276-282 comprising the
208 aforementioned Tyr277 and Thr280 residues involved in the binding of the coenzyme.
209 Electrostatic surface map calculations revealed that AGXT-1 would exhibit a higher density
210 and a different distribution of the surface charges with respect to hAGT1 (not shown).

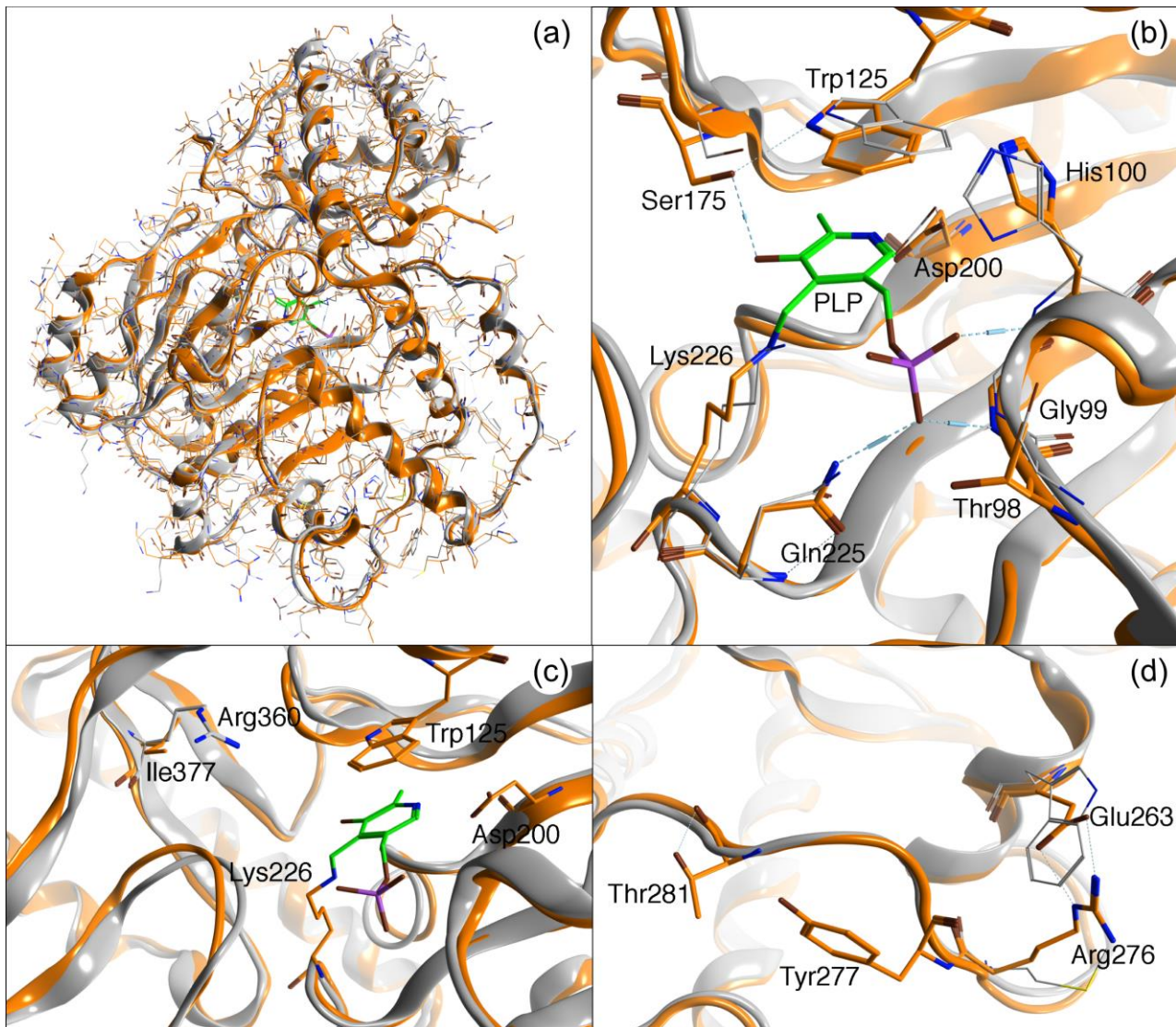


Figure 3. **Structural alignment of the AGXT-1 model with the hAGT1 structure.** Structural over imposition of AGXT-1 (orange) and hAGT1 (grey). The two backbones are represented as ribbons and the single residues as sticks. The PLP molecule is represented as green sticks.

211 **AGXT-1 is a dimeric PLP-dependent alanine:glyoxylate aminotransferase.** To
 212 compare the molecular properties of AGXT-1 and hAGT1, both recombinant proteins were
 213 expressed in and purified from *E. coli*. Along protein purification, size-exclusion
 214 chromatography analyses showed a single peak with similar retention volumes for both
 215 proteins and attributable to a dimer (82.6 ml and 84.9 ml in a Superdex™ 200 16/60 for
 216 hAGT1 and AGXT-1, respectively). Dynamic light scattering studies also revealed similar

217 hydrodynamic diameters for both proteins (8.1 ± 0.1 nm vs. 8.8 ± 0.4 nm, for hAGT1 and
218 AGXT-1, respectively), thus further confirming the dimeric assembly of the two proteins
219 [16,40]. As isolated, both proteins show spectroscopic features corresponding to PLP
220 bound to the active site by a Schiff base with Lys209 in hAGT1 and Lys226 in AGXT-1.
221 The UV-visible absorption and CD spectra of AGXT-1 display a band at 430 nm, which
222 likely reflects the ketoenamine tautomer of the internal Schiff base, and a band at 340 nm,
223 possibly corresponding to enolimine tautomer (Figure 4 and [6]). After incubation of AGXT-
224 1 with L-alanine, the spectra show almost no signal at 430 nm and a main absorption peak
225 and weak dichroic band at 340 nm (Figure 4). These signals indicate the formation of the
226 pyridoxamine-5'-phosphate (PMP) form of the coenzyme, thus supporting the proper
227 binding of PLP in the active site of AGXT-1 to take the amino group from the substrate L-
228 alanine. Attempts to remove the coenzyme from the active site of AGXT-1 (to obtain the
229 apo-form) by using the procedure applied for hAGT1 [16,17] yielded a form of AGXT-1
230 with PMP tightly bound, suggesting a very high affinity and/or very slow dissociation rate of
231 PMP. Further reduction of the pH (below 5.8) resulted in irreversible denaturation of
232 AGXT-1 before the release of the coenzyme, thus preventing a comparison between the
233 apo-form of AGXT-1 and hAGT1. Together, these results suggest that AGXT-1 binds PMP
234 with higher affinity than hAGT1 and/or that the pH value for efficient PMP release is lower
235 for AGXT-1.

236 Next, the ability of AGXT-1 to catalyse the amino transfer by using the natural
237 substrates of hAGT1 (L-alanine and glyoxylate) was tested (Figure 5). Activity data were
238 analysed by using a coupled enzyme assay as described for hAGT1 [6,16]. Kinetic
239 parameters for the overall transamination show that AGXT-1 has 5-fold higher activity
240 (V_{max}) than hAGT1 (Table 2), while apparent affinities (K_M) for both substrates are kept in
241 similar ranges. Only the apparent affinity for L-alanine is slightly higher (1.6-fold higher) for

242 AGXT-1 than for hAGT1. These results support a higher catalytic efficiency towards
 243 glyoxylate for the nematode enzyme than for the hAGT1. In addition, both proteins show
 244 similar dependence of the overall transaminase activity on temperature and pH (Figure 6).
 245 Arrhenius analyses of temperature dependence of transaminase activity reveal an
 246 activation energy value of $4.0 \pm 0.9 \text{ kcal} \cdot \text{mol}^{-1}$ for AGXT-1, somewhat higher than for
 247 hAGT1 ($2.2 \pm 1.8 \text{ kcal} \cdot \text{mol}^{-1}$) (Figure 6a). The activity of both enzymes decreases at mild
 248 acidic pH (Figure 6b-c), suggesting similar pattern of protonation states of the active site of
 249 both proteins, which could be a sign of similar reaction specificities [41] and environmental
 250 pH in their intracellular localization [42].

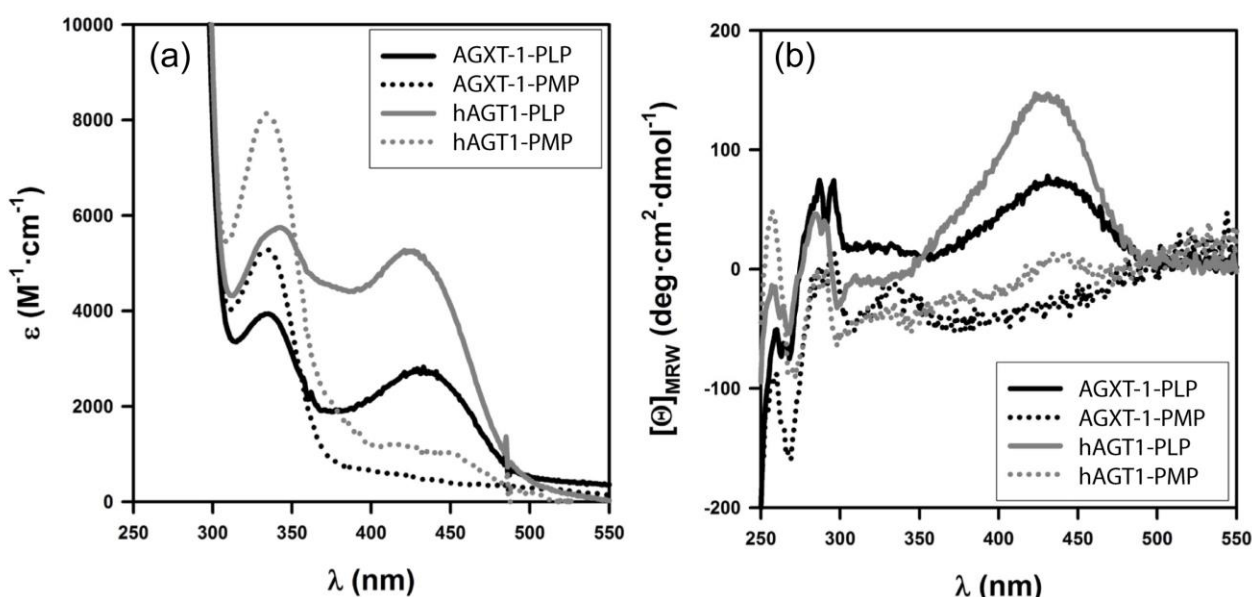


Figure 4. **Near-UV/visible spectroscopic analyses of AGXT-1 and hAGT1 in their PLP-bound forms and in the presence of 0.5 M L-alanine (PMP-forms).** (a) Near-UV/visible absorption spectra; (b) Near UV/visible circular dichroism spectra; Protein concentration was 20 μM in monomer.

Table 2. **Kinetic parameters of the overall transaminase activity for AGXT-1 and hAGT1.** Data are mean \pm s.d. from global fits from a coupled enzyme assay.

Parameter	AGXT-1	hAGT1
-----------	--------	-------

V_{\max} ($\text{mmol}\cdot\text{h}^{-1}\cdot\text{mg}^{-1}$)	11.3 ± 0.7	2.2 ± 0.1
$K_{M,\text{alanine}}$ (mM)	12 ± 2	20 ± 2
$K_{M,\text{glyoxylate}}$ (mM)	0.26 ± 0.05	0.26 ± 0.04

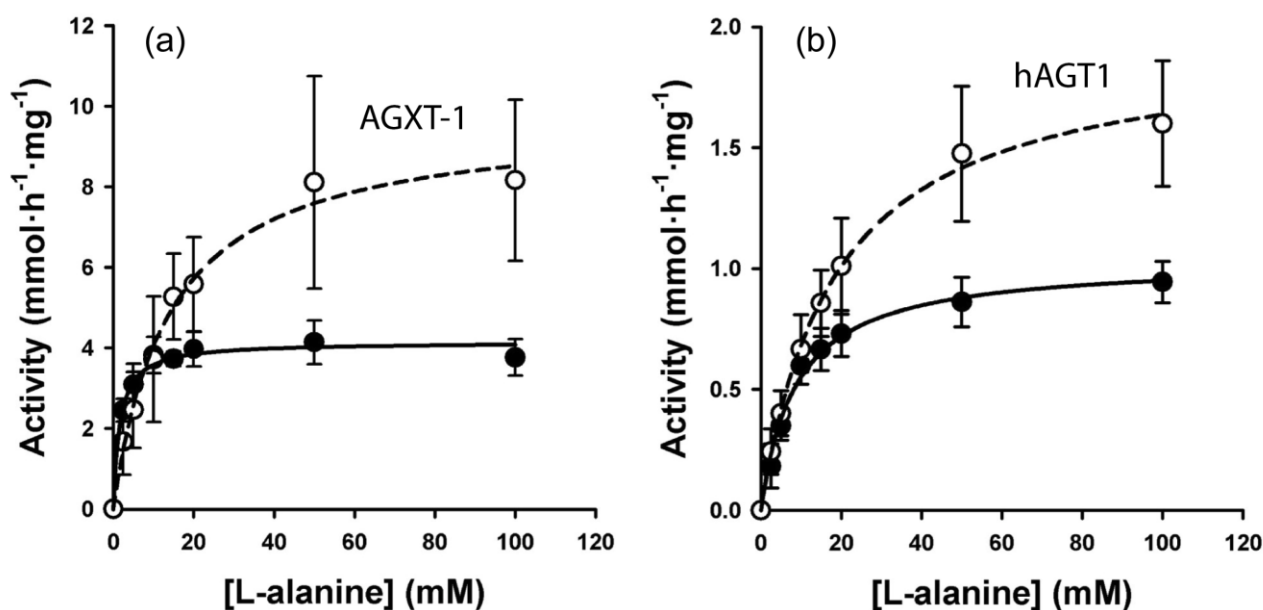


Figure 5. **Enzyme kinetic analyses of AGXT-1 (a) and hAGT1 (b) proteins in the presence of L-alanine and glyoxylate.** Experiments were performed at 0.25 mM (closed circles) and 2 mM (open circles) glyoxylate and varying L-alanine concentrations. Lines are global best-fits to an enzyme-substituted kinetic mechanism yielding the kinetic parameters shown in Table 2.

251 The large difference in activity between AGXT-1 and hAGT1 towards the
252 alanine:glyoxylate pair prompted us to investigate whether these two enzymes may share
253 similar substrate specificity [6]□. To this aim, we determined the specific activity of these
254 enzymes by using glyoxylate or pyruvate as amino acceptors and different natural L-amino
255 acids as amino donors (Figure 7). When using glyoxylate as amino acceptor, AGXT-1
256 protein is very specific towards L-alanine showing 300-fold and 130-fold higher activity
257 than for L-serine and L-phenylalanine and no detectable activity towards L-arginine, L-
258 glutamate and L-aspartate (Figure 7a). Under similar conditions, hAGT1 is somewhat less
259 specific, with 23-fold and 52-fold lower activity towards L-serine and L-arginine and 100-
260 fold and 200-fold lower activity towards L-phenylalanine and L-glutamate (Figure 7a).

261 Using pyruvate as amino acceptor (Figure 7b), both enzymes display lower activity
262 towards L-serine than those measured using glyoxylate. Their activities towards L-
263 phenylalanine are comparable, L-arginine is a better substrate for hAGT1 than AGXT-1
264 and L-glutamate and L-aspartate are poor substrates for both enzymes. Even though
265 some differences exist, these studies support similar substrate specificities for both
266 proteins and demonstrate that AGXT-1 protein is an alanine:glyoxylate aminotransferase.

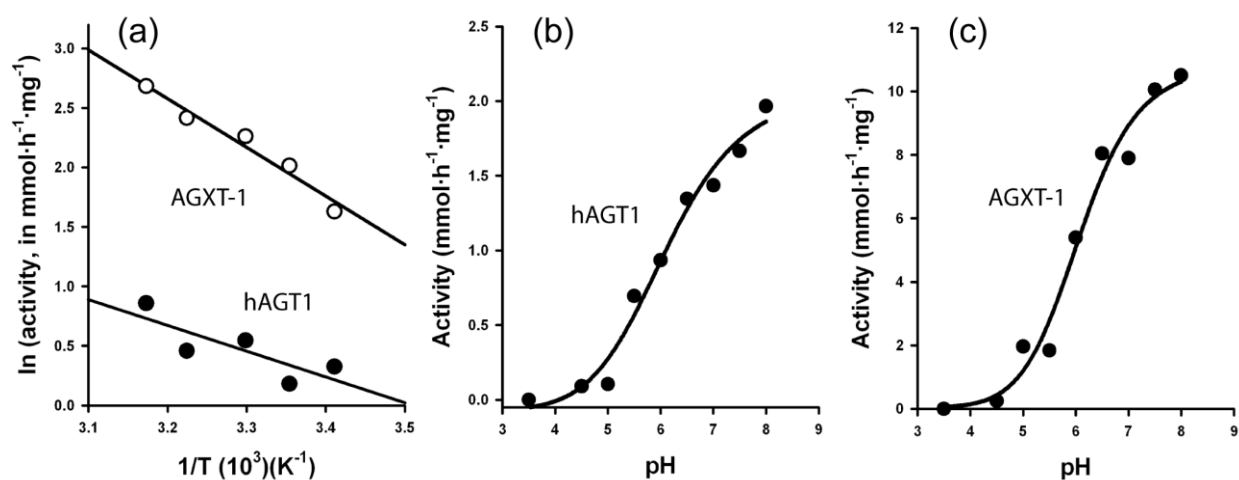


Figure 6. **Temperature- and pH-dependence of the overall transaminase activity for AGXT-1 and hAGT1 proteins.** (a) Arrhenius plots for the enzymatic activity of AGXT-1 and hAGT1; (b) and (c) pH-dependence of the enzymatic activity of hAGT1 and AGXT-1, respectively. Activity was measured in the presence of 100 mM L-alanine and 2 mM glyoxylate.

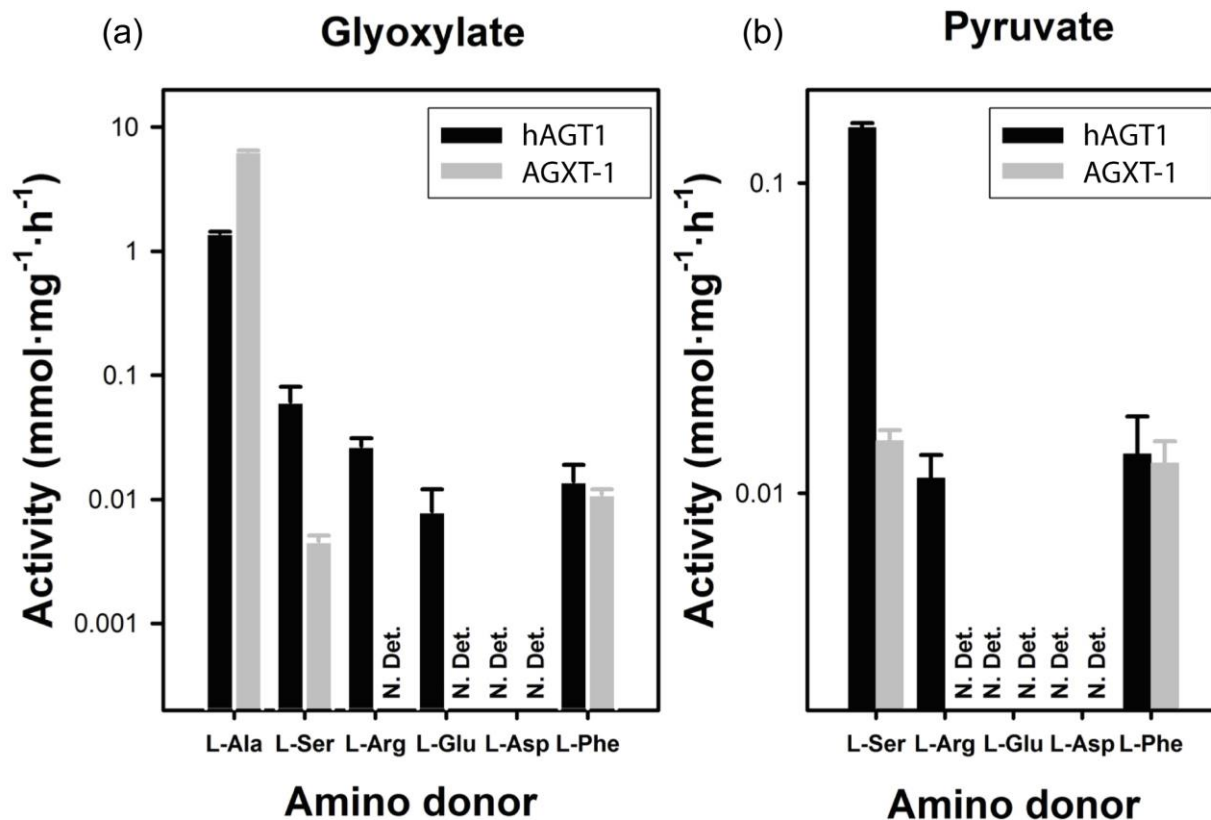


Figure 7. **Substrate specificity of AGXT-1 and hAGT1 towards different amino acids as amino donor using glyoxylate (a) or pyruvate (b) as amino acceptors.** The concentration of amino acids was 100 mM and of ketoacids was 2 mM. N.Det.- not detected.

267 **AGXT-1 shows lower resistance towards thermal and chemical denaturation.**

268 Thermal denaturation of AGXT-1 was studied by differential scanning calorimetry (DSC).

269 Both AGXT-1 and hAGT1 show a single denaturation transition (Figure 8a), which is well

270 described by a simple two-state irreversible denaturation model with first-order kinetics

271 (supported by protein concentration independent denaturation transitions [16,17] and data

272 not shown). The denaturation temperature (T_m) of AGXT-1 is about 12°C lower than that of

273 hAGT1 (Table 3). The lower denaturation enthalpy (ΔH) of AGXT-1 seems to be a

274 consequence of the lower thermal stability of this protein and a strongly temperature

275 dependent ΔH with a theoretical denaturation heat capacity of about 11 kcal·mol⁻¹·K⁻¹

276 (based on the correlations by [43]), thus suggesting that the amount of tertiary structure
 277 lost upon thermal denaturation in both enzymes is fairly similar. Due to the kinetic control
 278 of thermal denaturation for both enzymes, the DSC analyses can be used to extrapolate
 279 the denaturation rate constants to physiological temperatures (inset Figure 8a). The
 280 extrapolated kinetic stability for AGXT-1 towards thermal denaturation at 37°C is around
 281 200-fold lower than hAGT1 at this temperature (Table 3). However, when we compare the
 282 kinetic stability of both proteins at the corresponding physiological temperature (37°C for
 283 hAGT1 and 20°C for AGXT-1) the nematode protein is 90-fold more stable than hAGT1.

Table 3. **Thermal denaturation parameters for AGXT-1 and hAGT1.** The parameters have been determined from DSC scans using a two-state irreversible denaturation model. ¹ Data from Mesa-Torres, PLoS One, 2013. ² Determined at 3°C·min⁻¹ scan rate. ³ mean±s.d. from three different scan rates. ⁴ kinetic constant rates for irreversible denaturation extrapolated to 37°C (20°C)

Parameter	AGXT-1	hAGT1 ¹
T _m (°C) ²	69.8	82.1
ΔH (kcal·mol ⁻¹) ³	366±11	548±5
E _a (kcal·mol ⁻¹) ³	112±15	109±5
k _{37°C} (k _{20°C}) (min ⁻¹) ⁴	1.2·10 ⁻⁷ (7.1·10 ⁻¹²)	6.4·10 ⁻¹⁰

284 Urea induced denaturation of AGXT-1 was investigated by Far-UV circular
 285 dichroism spectroscopy (Figure 8b). Denaturation profiles of AGXT-1 and hAGT1 show a
 286 single transition and once again, AGXT-1 displays a lower stability with half-denaturation
 287 urea concentration of ~3.8 M (AGXT-1) vs. ~6 M (hAGT1). The cooperativity of urea-
 288 induced unfolding is apparently higher for AGXT-1 than for hAGT1. In contrast to hAGT1
 289 ([44] and data not shown), urea unfolding of AGXT-1 is highly reversible (Figure 8b
 290 squares). ~~indicating This reversibility suggests that, along the refolding pathway of AGXT-~~
 291 ~~1 upon chemical denaturation, the refolding pathway of AGXT-1 populates less population~~
 292 ~~of aggregation-prone intermediate states is much lower.~~

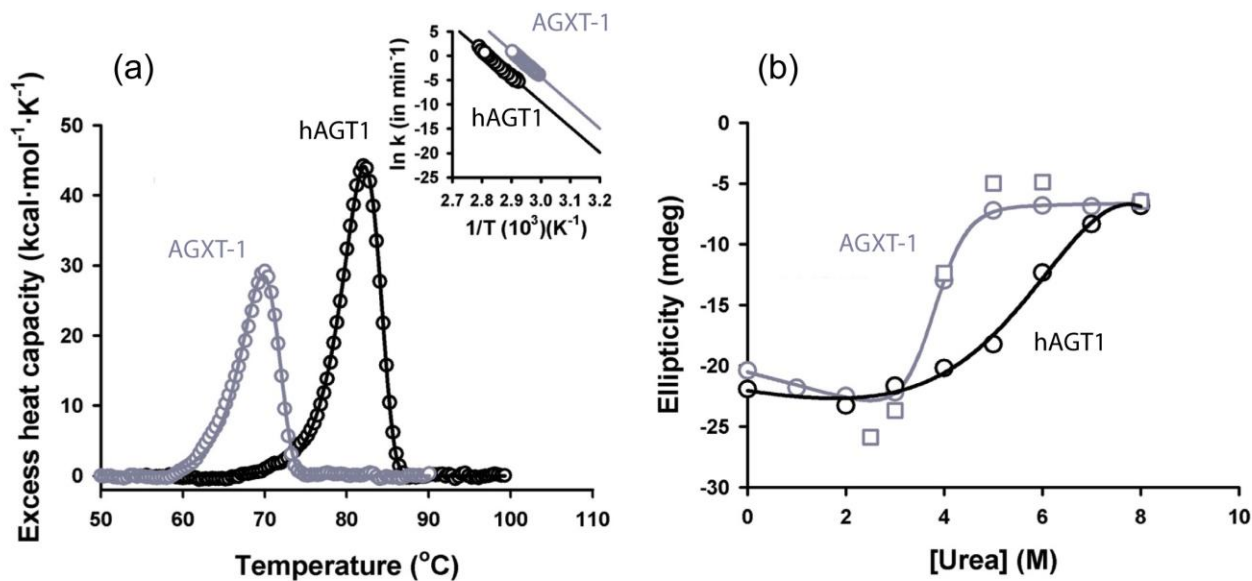


Figure 8. **Stability of AGXT-1 and hAGT1 proteins towards thermal and chemical denaturation.** (a) Thermal denaturation profiles of holo AGXT-1 and hAGT1 at 3°C·min⁻¹ and 5 μM protein subunit in 20 mM Na-Hepes, 200 mM NaCl pH 7.4. Lines are best-fits to a two-state irreversible model with first-order kinetics; Inset: Arrhenius plots for thermal denaturation kinetics; (b) Urea-induced unfolding of holo AGXT-1 and hAGT1 at 5 μM protein subunit in 20 mM Na-Hepes, 200 mM NaCl pH 7.4, 1 mM TCEP at 25°C. Circles show the results for unfolding, while squares correspond to refolding experiments.

293 4. Discussion

294 Glyoxylate is a metabolic intermediary in humans that has to be detoxified mainly by
 295 hAGT1 in peroxisomes [2]. Instead, glyoxylate is a key metabolite in *C. elegans* due to the
 296 presence of an active glyoxylate cycle [10,12]□. The sequencing of *C. elegans* genome
 297 predicted a putative ortholog of human AGXT gene in the nematode (ORF *T14D7.1*, [9]
 298 now renamed to *agxt-1*□). However, the molecular properties of the protein product of
 299 *agxt-1* gene have not been previously investigated. Here, we have performed a side-by-
 300 side comparative study on the molecular properties of AGXT-1 protein in comparison with
 301 human hAGT1, showing that AGXT-1 is a functional PLP-dependent enzyme with
 302 aminotransferase activity and a higher activity and specificity towards the
 303 alanine:glyoxylate pair than hAGT1. Our results also support that both enzymes are

304 structurally and functionally alike, but show different protein stability and subcellular
305 localization, where AGXT-1 is mitochondrial ~~whereas~~ and hAGT1 is peroxisomal.

306 The mitochondrial localization of AGXT-1 provides important insights into the
307 evolutionary adaptation of AGTs subcellular compartmentalization, and possibly, into its
308 relation with dietary origins of glyoxylate and the molecular origin of mitochondrial
309 mistargeting in PH1. AGT subcellular localization has represented a remarkable
310 conundrum for cell and evolutionary biologists and molecular pathologists. The AGTs
311 peroxisomal localization is attributed to a PTS1 located at the C-terminal domain, while the
312 mitochondrial localization is mainly controlled by the activation of a cryptic MTS in the N-
313 terminal domain that overrides the PTS1 route [1]. Therefore, the *AGXT* gene seems to
314 have evolved to meet dietary requirements, with alternative translation and transcription
315 sites to allow the protein to contain this strong MTS sequence [45]. In most omnivorous
316 mammals the AGT enzyme is distributed in mitochondria or peroxisomes, based on the
317 presence or absence of the MTS, respectively. In carnivorous mammals, the AGT
318 localization is mainly mitochondrial while a selective ~~lost~~ loss of the MTS is found in
319 herbivorous animals [46]. These evolutionary changes in subcellular distribution of AGT
320 associated with dietary changes have been recently exemplified by sequencing and
321 evolutionary analyses on different bat species with unparalleled dietary diversification [47].
322 Importantly, hAGT1 contains a very weak MTS, which becomes stronger in the presence
323 of the destabilizing P11L polymorphism and certain pathogenic mutations, that result into
324 mitochondrial mistargeting [16,48]. Unlike the behaviour found along evolution, which
325 seems to define the subcellular targeting of AGT using relatively simple transcriptional and
326 translational mechanisms, mitochondrial mistargeting of hAGT1 seems to depend strongly
327 on the cellular context. For instance, a given single genotype may lead or not to
328 mitochondrial import depending on the cell type and culture conditions [16,49,50]

329 highlighting the important role of molecular chaperones and/or other factors of the protein
330 homeostasis network in the final fate of hAGT1 disease-causing variants [16,17].

331 Along evolution, enzyme properties are selected to provide appropriate metabolic
332 rates at different physiological temperatures by tuning some structure-function
333 relationships i.e., stability, enzyme activity and ligand affinity [51]. While the physiological
334 temperature of humans is kept constant at 37°C, the nematode *C. elegans* is an ectotherm
335 organism that can survive between 8-27°C and whose physiology is highly affected by the
336 environmental temperature. The lower denaturation temperature and high catalytic activity
337 of AGXT-1 likely reflects coldtemperature-adaptation [52]. Moreover, the similar apparent
338 affinities for natural substrates of hAGT1 displayed by AGXT-1, suggest resemblance in
339 substrate concentration or K_M :[substrate] ratio, at their respective organelles [53]. It must
340 be noted that the activity and intracellular turnover of hAGT1 must be tuned to be
341 appropriate at a customarily constant temperature of 37°C, while the conformational
342 stability of AGXT-1 seems to be adapted to lower temperatures. These results may
343 indicate that the overall stability of different AGT orthologs is optimized to provide an
344 adequate intracellular turnover at optimal growth temperature, which in the case of hAGT1
345 is severely compromised by disease-associated mutations leading to protein misfolding
346 and mistargeting [2,16,40,54].

347 The main biological function of hAGT1 is to create a glyoxylate sink in peroxisomes of
348 of hepatocytes. In addition, there is a set of proteins that contribute to this human
349 glyoxylate metabolism. According to KEGG (Kyoto Encyclopedia of Genes and Genomes)
350 and REACTOME Pathway Database, these proteins are D-amino acid oxidase (hDAO),
351 hydroxyacid oxidase (hHAO), glyoxylate reductase / hydroxypyruvate reductase
352 (hGRHPR), D-4-hydroxy-2-oxoglutarate aldolase (hHOGA1), alanine:glyoxylate
353 aminotransferase 2 (hAGT2) and lactate dehydrogenase (hLDH) (Figure 9). Despite the

354 key role of glyoxylate cycle in *C. elegans* [55] (Figure 9), surprisingly the genome of the
355 nematode encodes orthologous proteins to those already described for the human
356 glyoxylate metabolism, with the only exception of mitochondrial hHOGA1 protein (

357 Table 4 (Table 4). Therefore the main routes of glyoxylate metabolism in humans are
358 expected to work in the nematode, at least to some extent. Some phenotypes have been
359 described by large-scale gene downregulation in *C. elegans*, such as the association of
360 C31C9.2 (ortholog of hGRHPR) [9] with low embryonic lethality [56] and slow growing [57],
361 or □ T09B4.8 (ortholog of hAGT2) linked to a reduction of fat content [58]. However,
362 according to the WormBase Consortium (www.wormbase.org - WS249) no altered
363 lethality, fertility or development has been described to the lack of function of AGXT-1,
364 F41E6.5 (ortholog of hDAO), DAAO1 and LDH-1 proteins. This suggests that the steps of
365 glyoxylate metabolism that are catalysed by these enzymes may not be essential for the
366 normal development and metabolism of the nematode. Nonetheless, the relative
367 contributions of these enzymes to different biochemical pathways requires knowledge on
368 their enzymatic properties and regulation, expression levels and metabolic fluxes, which
369 can be developmental and environmental dependent [59]. Alternatively, there are no
370 orthologous proteins in humans to the key *C. elegans* enzyme ICL-1, although a human
371 malate synthase activity has been detected with unknown biological function [60].

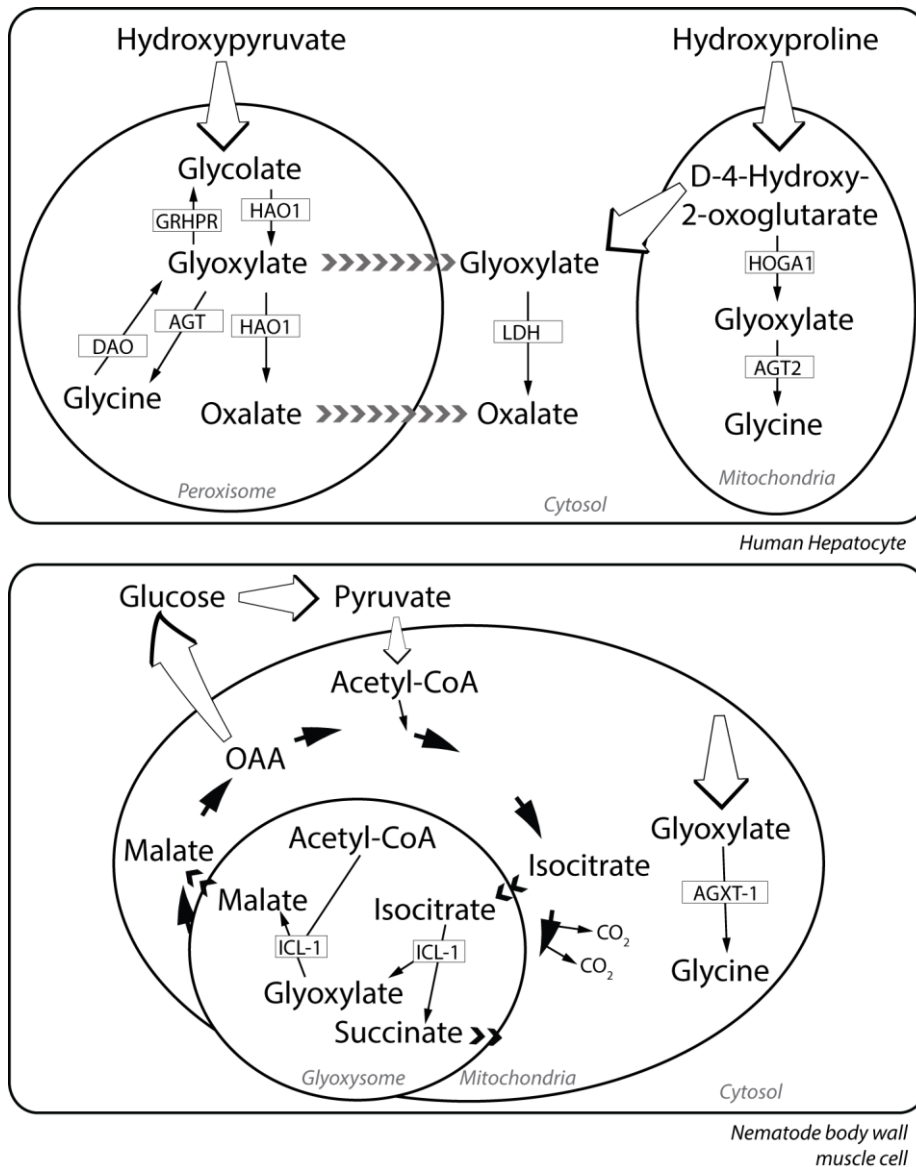


Figure 9. **Main routes of glyoxylate metabolism in human hepatocytes and nematode body wall muscle cells.** AGT: alanine:glyoxylate aminotransferase, DAO: D-amino acid oxidase, HAO1: hydroxyacid oxidase, GRHPR: glyoxylate reductase / hydroxyypyruvate reductase, HOGA1: D-4-hydroxy-2-oxoglutarate aldolase, AGT2: alanine:glyoxylate aminotransferase 2, LDH: lactate dehydrogenase and ICL-1: bi-functional isocitrate lyase:malate synthase.

372 In *C. elegans*, GC supports gluconeogenesis by incorporating acetyl-CoA (particularly from
 373 β -oxidation of fatty acids in peroxisome and mitochondria) and supplying succinate to TCA
 374 cycle and malate to the gluconeogenesis pathway [13,14]. The GC activity is increased
 375 during embryogenesis, L1 larvae and dauer diapause, while TCA cycle is increased in the

376 L2, L3 and L4 stages, when energy demands and food intake are increased [14]. The GC
377 and TCA cycles share some enzymatic activities (malate dehydrogenase, citrate synthase
378 and aconitase), while some enzymes, ICL-1 (GC) and isocitrate dehydrogenase (TCA),
379 compete for the same substrate (isocitrate). Therefore the relative activity of these
380 enzymes controls the ratio carbon flux through both cycles (GC and TCA) [55]. Unlike
381 other nematodes [61], evidence suggests that key enzymes of GC in *C. elegans* are
382 separable from mitochondria markers and may be compartmentalized in glyoxysome-like
383 microbodies [62]. This physical separation of GC and TCA enzymes may imply either the
384 existence of isoforms of those shared enzymes activities in glyoxysomes or the
385 transportation of metabolites (e.g., isocitrate and succinate) across organelles membranes
386 [63], which may function as a metabolic regulatory mechanism [64]. The existence of a
387 highly active alanine:glyoxylate aminotransferase (AGXT-1) in the mitochondria of the
388 nematode could avoid the competition with ICL-1 enzyme for the substrate glyoxylate. The
389 transamination of glyoxylate into glycine could provide a way to modulate levels of
390 glyoxylate in mitochondria, which would otherwise be toxic and may affect the regulation of
391 the TCA cycle by inhibiting enzymes such as ketoglutarate dehydrogenase [65]. In
392 humans, the hAGT1 activity is known to act in the detoxification of glyoxylate within
393 peroxisomes of hepatocytes, while the presence of an active glyoxylate cycle in the
394 nematode opens the possibility of alternative metabolic roles for the AGXT-1 protein. To
395 further characterize the role of AGXT-1 on different metabolic pathways and
396 developmental conditions, combined RNAi downregulation of both *agxt-1* and *icl-1* genes
397 as well as the generation of *agxt-1;icl-1* double mutant with analyses of metabolites in *C.*
398 *elegans* cultures should be approached.

Table 4. **Orthologous proteins in *C. elegans* found from a BLASTP of human proteins involved in glyoxylate metabolism.** GI numbers of protein sequence used are: hAGT- 126522481; hDAO- 148539837; hHAO- 11068137; hGRHPR- 6912396; hHOGA- 31543060; hAGT2- 119576316; hLDH- 32693754. n/a, not available.

<i>H. sapiens</i>			<i>C. elegans</i>			
Protein	Residues	Localization	Protein	Residues	Identity	E value
hAGT	392	Perox.	AGXT-1	405	44%	$5 \cdot 10^{-115}$
hDAO	347	Perox.	DAAO1	322	35%	$8 \cdot 10^{-61}$
hHAO	370	Perox.	F41E6.5b	371	46%	$6 \cdot 10^{-115}$
hGRHPR	328	Perox./Cyt.	C31C9.2	322	30%	$1 \cdot 10^{-29}$
hHOGA	327	Mito.	Not found	n/a	n/a	n/a
hAGT2	514	Mito.	T09B4.8	444	53%	$1 \cdot 10^{-165}$
hLDH	332	Cyt.	LDH-1	333	54%	$6 \cdot 10^{-119}$

399 *C. elegans* is a remarkably useful model system to understand protein folding
400 diseases and their pharmacological correction [66–68]. Our studies pave the way to
401 develop suitable models for PH1 using *C. elegans*. To generate them, it will be important
402 to determine whether simultaneous inactivation of *agxt-1* gene and the malate synthase
403 domain of ICL-1 make the nematodes susceptible to glyoxylate toxicity, similarly to what is
404 found in humans with hAGT1 deficiency. Alternatively, models expressing disease-
405 associated variants of hAGT1 in *C. elegans* may also provide a convenient *in vivo* platform
406 to explore and dissect the complex protein homeostasis defects associated with PH1-
407 causing mutations.

Acknowledgments.

We thank Prof. Jose Manuel Sanchez-Ruiz for support. This work was supported by the Spanish Ministry of Science and Innovation (CSD2009-00088, BIO2012-34937 and SAF2011-23933), Junta de Andalucia (P11-CTS-7187), FEDER Funds and the Oxalosis and Hyperoxaluria Foundation (to B.C.). A. L. P. acknowledges a Ramon y Cajal research contract (RyC2009-04147) from the Spanish ministry of Science and Innovation and the University of Granada. N. M-T acknowledges a FPI predoctoral fellowship from the Spanish Ministry of Science and Innovation. A.C.C. and N.T. were supported by the grant IOS-1353845 from the National Science Foundation (NSF). N.T. acknowledges the Tetelman Fellowship for International Research on the Sciences awarded by Yale University.

References

- [1] Danpure CJ. Variable peroxisomal and mitochondrial targeting of alanine: glyoxylate aminotransferase in mammalian evolution and disease. *Bioessays* 1997;19:317–26. doi:10.1002/bies.950190409.
- [2] Salido E, Pey AL, Rodriguez R, Lorenzo V. Primary hyperoxalurias: disorders of glyoxylate detoxification. *Biochim Biophys Acta* 2012;1822:1453–64. doi:10.1016/j.bbadis.2012.03.004.
- [3] Baker PRS, Cramer SD, Kennedy M, Assimios DG, Holmes RP. Glycolate and glyoxylate metabolism in HepG2 cells. *Am J Physiol Cell Physiol* 2004;287:C1359–65. doi:10.1152/ajpcell.00238.2004.
- [4] Caplin B, Wang Z, Slaviero A, Tomlinson J, Dowsett L, Delahaye M, et al. Alanine-glyoxylate aminotransferase-2 metabolizes endogenous methylarginines, regulates NO, and controls blood pressure. *Arter Thromb Vasc Biol* 2012;32:2892–900. doi:10.1161/ATVBAHA.112.254078.
- [5] Rodionov RN, Jarzebska N, Weiss N, Lentz SR. AGXT2: a promiscuous aminotransferase. *Trends Pharmacol Sci* 2014;35:575–82. doi:10.1016/j.tips.2014.09.005.

- [6] Cellini B, Bertoldi M, Montioli R, Paiardini A, Borri Voltattorni C. Human wild-type alanine:glyoxylate aminotransferase and its naturally occurring G82E variant: functional properties and physiological implications. *Biochem J* 2007;408:39–50. doi:10.1042/BJ20070637.
- [7] Oppici E, Montioli R, Cellini B. Liver peroxisomal alanine:glyoxylate aminotransferase and the effects of mutations associated with Primary Hyperoxaluria Type I: An overview. *Biochim Biophys Acta* 2015;1854:1212–9. doi:10.1016/j.bbapap.2014.12.029.
- [8] *C. elegans* Sequencing Consortium. Genome sequence of the nematode *C. elegans*: a platform for investigating biology. *Science* (80-) 1998;282:2012–8.
- [9] Kuwabara PE, O’Neil N. The use of functional genomics in *C. elegans* for studying human development and disease. *J Inherit Metab Dis* 2001;24:127–38.
- [10] Colonna WJ, McFadden BA. Isocitrate lyase from parasitic and free-living nematodes. *Arch Biochem Biophys* 1975;170:608–19.
- [11] Kornberg HL, Madsen NB. Synthesis of C4-dicarboxylic acids from acetate by a glyoxylate bypass of the tricarboxylic acid cycle. *Biochim Biophys Acta* 1957;24:651–3.
- [12] Liu F, Thatcher JD, Barral JM, Epstein HF. Bifunctional glyoxylate cycle protein of *Caenorhabditis elegans*: a developmentally regulated protein of intestine and muscle. *Dev Biol* 1995;169:399–414. doi:10.1006/dbio.1995.1156.
- [13] Khan FR, McFadden BA. *Caenorhabditis elegans*: decay of isocitrate lyase during larval development. *Exp Parasitol* 1982;54:47–54.
- [14] Wadsworth WG, Riddle DL. Developmental regulation of energy metabolism in *Caenorhabditis elegans*. *Dev Biol* 1989;132:167–73.
- [15] Pace CN, Vajdos F, Fee L, Grimsley G, Gray T. How to measure and predict the molar absorption coefficient of a protein. *Protein Sci* 1995;4:2411–23. doi:10.1002/pro.5560041120.
- [16] Mesa-Torres N, Fabelo-Rosa I, Riverol D, Yunta C, Albert A, Salido E, et al. The Role of Protein Denaturation Energetics and Molecular Chaperones in the Aggregation and Mistargeting of Mutants Causing Primary Hyperoxaluria Type I. *PLoS One* 2013;8:e71963.
- [17] Pey AL, Salido E, Sanchez-Ruiz JM. Role of low native state kinetic stability and interaction of partially unfolded states with molecular chaperones in the

mitochondrial protein mistargeting associated with primary hyperoxaluria. *Amino Acids* 2011;41:1233–45. doi:10.1007/s00726-010-0801-2.

- [18] Peterson EA, Sober HA. Preparation of Crystalline Phosphorylated Derivatives of Vitamin B6. *J Am Chem Soc* 1954;76:169–75. doi:10.1021/ja01630a045.
- [19] Rumsby G, Weir T, Samuel CT. A semiautomated alanine:glyoxylate aminotransferase assay for the tissue diagnosis of primary hyperoxaluria type 1. *Ann Clin Biochem* 1997;34 (Pt 4):400–4.
- [20] Cellini B, Bertoldi M, Borri Voltattorni C. *Treponema denticola* cystalysin catalyzes beta-desulfination of L-cysteine sulfinic acid and beta-decarboxylation of L-aspartate and oxalacetate. *FEBS Lett* 2003;554:306–10.
- [21] Sánchez-Ruiz JM, López-Lacomba JL, Cortijo M, Mateo PL. Differential scanning calorimetry of the irreversible thermal denaturation of thermolysin. *Biochemistry* 1988;27:1648–52.
- [22] Brenner S. The Genetics of *Caenorhabditis elegans*. *Genetics* 1974;77:71–94.
- [23] Mello C, Fire A. DNA transformation. *Methods Cell Biol* 1995;48:451–82.
- [24] Zhang X, Roe SM, Hou Y, Bartlam M, Rao Z, Pearl LH, et al. Crystal structure of alanine:glyoxylate aminotransferase and the relationship between genotype and enzymatic phenotype in primary hyperoxaluria type 1. *J Mol Biol* 2003;331:643–52.
- [25] Neupert W. Protein import into mitochondria. *Annu Rev Biochem* 1997;66:863–917. doi:10.1146/annurev.biochem.66.1.863.
- [26] Claros MG, Vincens P. Computational method to predict mitochondrially imported proteins and their targeting sequences. *Eur J Biochem* 1996;241:779–86.
- [27] Emanuelsson O, Brunak S, von Heijne G, Nielsen H. Locating proteins in the cell using TargetP, SignalP and related tools. *Nat Protoc* 2007;2:953–71. doi:10.1038/nprot.2007.131.
- [28] Motley A, Lumb MJ, Oatey PB, Jennings PR, De Zoysa PA, Wanders RJ, et al. Mammalian alanine:glyoxylate aminotransferase 1 is imported into peroxisomes via the PTS1 translocation pathway. Increased degeneracy and context specificity of the mammalian PTS1 motif and implications for the peroxisome-to-mitochondrion mistargeting of . *J Cell Biol* 1995;131:95–109.

- [29] Knott TG, Birdsey GM, Sinclair KE, Gallagher IM, Purdue PE, Danpure CJ. The peroxisomal targeting sequence type 1 receptor, Pex5p, and the peroxisomal import efficiency of alanine:glyoxylate aminotransferase. *Biochem J* 2000;352 Pt 2:409–18.
- [30] Petriv OI, Pilgrim DB, Rachubinski R a, Titorenko VI. RNA interference of peroxisome-related genes in *C. elegans*: a new model for human peroxisomal disorders. *Physiol Genomics* 2002;10:79–91. doi:10.1152/physiolgenomics.00044.2002.
- [31] Motley AM, Hettema EH, Ketting R, Plasterk R, Tabak HF. *Caenorhabditis elegans* has a single pathway to target matrix proteins to peroxisomes. *EMBO Rep* 2000;1:40–6. doi:10.1038/sj.embor.embor626.
- [32] Sievers F, Wilm A, Dineen D, Gibson TJ, Karplus K, Li W, et al. Fast, scalable generation of high-quality protein multiple sequence alignments using Clustal Omega. *Mol Syst Biol* 2011;7:539. doi:10.1038/msb.2011.75.
- [33] McKay SJ, Johnsen R, Khattra J, Asano J, Baillie DL, Chan S, et al. Gene expression profiling of cells, tissues, and developmental stages of the nematode *C. elegans*. *Cold Spring Harb Symp Quant Biol* 2003;68:159–69.
- [34] Dupuy D, Bertin N, Hidalgo CA, Venkatesan K, Tu D, Lee D, et al. Genome-scale analysis of in vivo spatiotemporal promoter activity in *Caenorhabditis elegans*. *Nat Biotechnol* 2007;25:663–8. doi:10.1038/nbt1305.
- [35] Meissner B, Rogalski T, Viveiros R, Warner A, Plastino L, Lorch A, et al. Determining the sub-cellular localization of proteins within *Caenorhabditis elegans* body wall muscle. *PLoS One* 2011;6:e19937. doi:10.1371/journal.pone.0019937.
- [36] Fares H, van der Bliek AM. Analysis of membrane-bound organelles. *Methods Cell Biol* 2012;107:239–63. doi:10.1016/B978-0-12-394620-1.00008-4.
- [37] Curran SP, Leverich EP, Koehler CM, Larsen PL. Defective mitochondrial protein translocation precludes normal *Caenorhabditis elegans* development. *J Biol Chem* 2004;279:54655–62. doi:10.1074/jbc.M409618200.
- [38] Billing O, Kao G, Naredi P. Mitochondrial function is required for secretion of DAF-28/insulin in *C. elegans*. *PLoS One* 2011;6:e14507. doi:10.1371/journal.pone.0014507.
- [39] Montioli R, Roncador A, Oppici E, Mandrile G, Giachino DF, Cellini B, et al. S81 L and G170R mutations causing Primary Hyperoxaluria Type I in homozygosis and

heterozygosis: an example of positive interallelic complementation. *Hum Mol Genet* 2014. doi:10.1093/hmg/ddu329.

- [40] Cellini B, Montioli R, Voltattorni CB. Human liver peroxisomal alanine:glyoxylate aminotransferase: characterization of the two allelic forms and their pathogenic variants. *Biochim Biophys Acta* 2011;1814:1577–84. doi:10.1016/j.bbapap.2010.12.005.
- [41] Toney MD. Controlling reaction specificity in pyridoxal phosphate enzymes. *Biochim Biophys Acta* 2011;1814:1407–18. doi:10.1016/j.bbapap.2011.05.019.
- [42] Chan P, Warwicker J. Evidence for the adaptation of protein pH-dependence to subcellular pH. *BMC Biol* 2009;7:69. doi:10.1186/1741-7007-7-69.
- [43] Robertson AD, Murphy KP. Protein Structure and the Energetics of Protein Stability. *Chem Rev* 1997;97:1251–68.
- [44] Cellini B, Lorenzetto A, Montioli R, Oppici E, Voltattorni CB. Human liver peroxisomal alanine:glyoxylate aminotransferase: Different stability under chemical stress of the major allele, the minor allele, and its pathogenic G170R variant. *Biochimie* 2010;92:1801–11. doi:10.1016/j.biochi.2010.08.005.
- [45] Birdsey GM, Lewin J, Cunningham AA, Bruford MW, Danpure CJ. Differential enzyme targeting as an evolutionary adaptation to herbivory in carnivora. *Mol Biol Evol* 2004;21:632–46. doi:10.1093/molbev/msh054.
- [46] Danpure CJ, Fryer P, Jennings PR, Allsop J, Griffiths S, Cunningham A. Evolution of alanine:glyoxylate aminotransferase 1 peroxisomal and mitochondrial targeting. A survey of its subcellular distribution in the livers of various representatives of the classes Mammalia, Aves and Amphibia. *Eur J Cell Biol* 1994;64:295–313.
- [47] Liu Y, Xu H, Yuan X, Rossiter SJ, Zhang S. Multiple adaptive losses of alanine-glyoxylate aminotransferase mitochondrial targeting in fruit-eating bats. *Mol Biol Evol* 2012;29:1507–11. doi:10.1093/molbev/mss013.
- [48] Purdue PE, Allsop J, Isaya G, Rosenberg LE, Danpure CJ. Mistargeting of peroxisomal L-alanine:glyoxylate aminotransferase to mitochondria in primary hyperoxaluria patients depends upon activation of a cryptic mitochondrial targeting sequence by a point mutation. *Proc Natl Acad Sci U S A* 1991;88:10900–4.
- [49] Santana A, Salido E, Torres A, Shapiro LJ. Primary hyperoxaluria type 1 in the Canary Islands: a conformational disease due to I244T mutation in the P11L-

containing alanine:glyoxylate aminotransferase. *Proc Natl Acad Sci U S A* 2003;100:7277–82. doi:10.1073/pnas.1131968100.

- [50] Fargue S, Lewin J, Rumsby G, Danpure CJ. Four of the most common mutations in primary hyperoxaluria type 1 unmask the cryptic mitochondrial targeting sequence of alanine:glyoxylate aminotransferase encoded by the polymorphic minor allele. *J Biol Chem* 2013;288:2475–84. doi:10.1074/jbc.M112.432617.
- [51] Somero GN. Adaptation of enzymes to temperature: searching for basic “strategies.” *Comp Biochem Physiol B Biochem Mol Biol* 2004;139:321–33. doi:10.1016/j.cbpc.2004.05.003.
- [52] Somero GN. Proteins and temperature. *Annu Rev Physiol* 1995;57:43–68. doi:10.1146/annurev.ph.57.030195.000355.
- [53] Somero GN. Temperature adaptation of enzymes: biological optimization through structure-function compromises. *Annu Rev Ecol Syst* 1978;9:1–29.
- [54] Oppici E, Montioli R, Lorenzetto A, Bianconi S, Borri Voltattorni C, Cellini B. Biochemical analyses are instrumental in identifying the impact of mutations on holo and/or apo-forms and on the region(s) of alanine:glyoxylate aminotransferase variants associated with primary hyperoxaluria type I. *Mol Genet Metab* 2012;105:132–40. doi:10.1016/j.ymgme.2011.09.033.
- [55] O’Riordan VB, Burnell AM. Intermediary metabolism in the dauer larva of the nematode *Caenorhabditis elegans* - II. The glyoxylate cycle and fatty-acid oxidation. *Comp Biochem Physiol Part B Comp Biochem* 1990;95:125–30.
- [56] Maeda I, Kohara Y, Yamamoto M, Sugimoto A. Large-scale analysis of gene function in *Caenorhabditis elegans* by high-throughput RNAi. *Curr Biol* 2001;11:171–6.
- [57] Hanazawa M, Mochii M, Ueno N, Kohara Y, Iino Y. Use of cDNA subtraction and RNA interference screens in combination reveals genes required for germ-line development in *Caenorhabditis elegans*. *Proc Natl Acad Sci U S A* 2001;98:8686–91. doi:10.1073/pnas.141004698.
- [58] Ashrafi K, Chang FY, Watts JL, Fraser AG, Kamath RS, Ahringer J, et al. Genome-wide RNAi analysis of *Caenorhabditis elegans* fat regulatory genes. *Nature* 2003;421:268–72. doi:10.1038/nature01279.
- [59] Braeckman BP, Houthoofd K, Vanfleteren JR. Intermediary metabolism. *WormBook* 2009:1–24. doi:10.1895/wormbook.1.146.1.

- [60] Strittmatter L, Li Y, Nakatsuka NJ, Calvo SE, Grabarek Z, Mootha VK. CLYBL is a polymorphic human enzyme with malate synthase and beta-methylmalate synthase activity. *Hum Mol Genet* 2014. doi:10.1093/hmg/ddt624.
- [61] Rubin H, Trelease RN. Subcellular localization of glyoxylate cycle enzymes in *Ascaris suum* larvae. *J Cell Biol* 1976;70:374–83.
- [62] Patel TR, McFadden BA. Particulate isocitrate lyase and malate synthase in *Caenorhabditis elegans*. *Arch Biochem Biophys* 1977;183:24–30.
- [63] Kunze M, Pracharoenwattana I, Smith SM, Hartig A. A central role for the peroxisomal membrane in glyoxylate cycle function. *Biochim Biophys Acta* 2006;1763:1441–52. doi:10.1016/j.bbamcr.2006.09.009.
- [64] Bolla R, Zuckerman BM, others. Nematode energy metabolism. *Nematodes as Biol Model Vol 2 Aging Other Model Syst* 1980:165–92.
- [65] Adinolfi A, Moratti R, Olezza S, Ruffo A. Control of the citric acid cycle by glyoxylate. The mechanism of inhibition of oxoglutarate dehydrogenase, isocitrate dehydrogenase and aconitate hydratase. *Biochem J* 1969;114:513–8.
- [66] Calamini B, Morimoto RI. Protein homeostasis as a therapeutic target for diseases of protein conformation. *Curr Top Med Chem* 2012;12:2623–40.
- [67] Silva MC, Fox S, Beam M, Thakkar H, Amaral MD, Morimoto RI. A genetic screening strategy identifies novel regulators of the proteostasis network. *PLoS Genet* 2011;7:e1002438. doi:10.1371/journal.pgen.1002438.
- [68] Casanueva MO, Burga A, Lehner B. Fitness trade-offs and environmentally induced mutation buffering in isogenic *C. elegans*. *Science* (80-) 2012;335:82–5. doi:10.1126/science.1213491.